

DETERMINATION OF THE VISUAL ORBIT OF THE SPECTROSCOPIC BINARY  
 $\alpha$  ANDROMEDAE WITH SUBMILLIARCSECOND PRECISION

XIAOPEI PAN

Department of Astronomy, California Institute of Technology, Pasadena, CA 91125

MICHAEL SHAO AND M. MARK COLAVITA

Optical Sciences and Application Section, Jet Propulsion Laboratory, Pasadena, CA 91109

AND

J. THOMAS ARMSTRONG,<sup>1</sup> DAVID MOZURKEWICH,<sup>2</sup> MADDALI VIVEKANAND,<sup>1</sup> CRAIG S. DENISON,<sup>3</sup>  
RICHARD S. SIMON,<sup>4</sup> AND KENNETH J. JOHNSTON<sup>2</sup>

NRL/USNO Optical Interferometer Project, US Naval Observatory, Washington, DC 20392

Received 1991 April 12; accepted 1991 May 31

## ABSTRACT

The visual orbit of the spectroscopic binary  $\alpha$  And has been determined independently of spectroscopic data using the Mark III Stellar Interferometer. Observations of  $\alpha$  And in 1988 and 1989 clearly demonstrate submilliarcsecond measurement precision at optical wavelengths. All of the orbital elements of  $\alpha$  And have been calculated utilizing observations from the Mark III Stellar Interferometer only and are in excellent agreement with the spectroscopic results. However, three of these elements, i.e.,  $a''$ ,  $i$ , and  $\Omega$ , can only be obtained from interferometric data. Using both interferometric and spectroscopic observations, the definitive orbital elements are determined as follows: angular semimajor axis  $a'' = 0''.02415 \pm 0''.00013$ , inclination  $i = 105^\circ.66 \pm 0^\circ.22$ , position angle of ascending node  $\Omega = 104^\circ.16 \pm 0^\circ.25$ , longitude of periastron  $\omega = 77^\circ.31 \pm 0^\circ.32$ , period  $P = 96^d.6960 \pm 0^d.0013$ , eccentricity  $e = 0.527 \pm 0.004$ , and epoch of periastron passage  $T = \text{JD } 2,447,374.77 \pm 0.15$ . In addition, the magnitude difference between the two components has been measured, yielding  $\Delta m = 1.82 \pm 0.04$  mag at 800 nm and  $\Delta m = 1.99 \pm 0.04$  mag at 550 nm. Incorporating photometric observations, the color indices between 550 nm and 800 nm for the primary and the companion are determined as  $-0.11 \pm 0.03$  mag and  $+0.07 \pm 0.05$  mag, respectively.

*Subject headings:* binaries: visual — instrumentation: interferometers — stars: individual ( $\alpha$  Andromedae)

## 1. INTRODUCTION

The Mark III Stellar Interferometer, located on Mount Wilson, California, has been used initially to measure star positions and stellar diameters. A series of papers has been published describing the instrument (Shao et al. 1988), two-color astrometry (Colavita, Shao, & Staelin 1987), star position determination (Mozurkewich et al. 1988; Shao et al. 1990), and stellar diameter measurement (Shao et al. 1987; Hutter et al. 1989; Mozurkewich et al. 1991). The observation program of binary systems started in 1988 (cf. Pan et al. 1990).

For binary observations, a variable baseline is used, which provides 36 different lengths from 3 to 32 m oriented N-S. Fringes are observed simultaneously in four spectral channels: a wide-band channel at 700 nm for fringe tracking, and three narrow-band channels with typical center wavelengths of 800, 550, and 450 nm. Because of low signal-to-noise ratio at 450 nm, the data from this channel were not used here. The bandwidths of the 800 and 550 nm channels, which were analyzed, were 22 and 25 nm, respectively. The aperture for the narrow-band channels was usually 2.5 cm. Each scan of a star includes fringe-tracking data recorded over a 75 s interval, followed by a 5 s measurement of the total dark count and sky background.

Selected reference stars with diameters equal to or smaller than 1 mas are observed periodically during the night.

The Mark III Stellar Interferometer is a fully automated instrument. At the beginning of each night, an observation list is loaded by an observer. For each scan, the siderostats and delay lines slew to the target star. After the angle tracker has acquired and locked on the star, fringe acquisition begins. Under normal seeing conditions, fringes can be acquired in a few seconds. After recording fringe-tracking data over a period of 75 s, the siderostats are offset for a measurement of the total dark count and sky background. A scan typically takes 3 minutes, and a total of 160–200 scans can be made each night. Usually, 15–25 scans per night are scheduled for each binary star.

In this paper, data reduction of the binary star observations will be described first. The observations on  $\alpha$  And are presented next. The orbital elements of this system are then calculated using interferometric data only and are compared with the results from spectroscopy. Predictions of the orbital motion of  $\alpha$  And are made and are compared with measurement data. The magnitude difference of this system at different wavelengths is also presented. Finally, the implications of these results on the physical parameters of the system are described.

<sup>1</sup> Postal address: Universities Space Research Associates, Washington, DC 20024.

<sup>2</sup> Postal address: Center for Advanced Space Sensing, Naval Research Laboratory, Washington, DC 20375.

<sup>3</sup> Postal address: SFA Inc., Landover, MD 20785.

<sup>4</sup> Postal address: Interferometrics, Inc., Vienna, VA 22182.

## 2. DATA REDUCTION OF BINARY STAR OBSERVATIONS

Analysis of the interferometric data for the study of binary star systems is divided into four steps, discussed below.

### 2.1. Calculation of the Fringe Visibility

The basic frame rate for data recording with the Mark III interferometer is 4 ms. In the initial processing, the fringe parameters are calculated and averaged to 0.5 s. The squared fringe visibility<sup>5</sup>,  $V^2$ , is calculated for each 0.5 s period using the unbiased estimator

$$V^2 = (\pi^2/2) \langle (A-C)^2 + (B-D)^2 - N \rangle / \langle N - D_r \rangle^2, \quad (1)$$

where  $A$ ,  $B$ ,  $C$ , and  $D$  are the number of detected photons in each of four time bins during the path-length modulation stroke;  $N = A + B + C + D$  is the total number of photons per frame;  $D_r$  is the total dark count and sky background correction normalized to 4 ms; and  $\langle \dots \rangle$  denotes a time average over 126 frames (cf. Shao et al. 1988). The bin widths in each channel are adjusted electronically so that the effective path-length stroke is matched to the center wavelength.

On the basis of the dark count and sky background measurements, data during twilight at the beginning and end of each night are discarded. Dark count measurements over the remaining interval are then edited to remove erroneous points: measurements exceeding  $3\sigma$  are discarded. The average of the nearest five dark count measurements is then used as the correction in the previous expression.

In order to avoid errors in fringe visibility measurements caused by, for example, radio frequency interference in the detector electronics, a data qualification step is taken here. The variance of the photon flux in each frame is given by the sum of a photon noise term and an atmospheric scintillation term; for the visibility channels, because of the relatively low number of photons per frame, the photon noise term dominates. Since photon noise has a Poisson distribution, its standard deviation is given by  $\sigma = N^{1/2}$ . We discard those frames whose photon count exceeds the mean value by  $5\sigma$  or more. This is the only criterion we adopted to reject data points.

After this qualification step, the 0.5 s  $V^2$  measurements are integrated to 5 s. These 5 s points are averaged to a scan ( $\sim 75$  s), and the rms of the 5 s points within the scan is used as an estimate of the measurement error of the scan  $\sigma_{\text{scan}}$ .

### 2.2. Determination of Projected Baseline and Effective Wavelengths

For a two-element interferometer, the fringe position  $D$  is given by  $D = B \cdot s + C$ , where  $B$  is the baseline vector,  $s$  is the unit vector to the star, and  $C$  is the delay offset, representing the zero point of the laser metrology system. The two components of the projected baseline vector on the  $u$ - $v$  plane are calculated as

$$B_u = B_x \sin h - B_y \cos h, \quad (2)$$

$$B_v = -B_x \sin \delta \cos h - B_y \sin \delta \sin h + B_z \cos \delta, \quad (3)$$

where  $B_x$ ,  $B_y$ , and  $B_z$  are the three components of the baseline vector in the equatorial coordinate system, and  $\delta$  and  $h$  are the declination and hour angle of the star.

In order to perform a first-order correction for the bias caused by the finite bandwidth of the filters, we approximate the stellar spectrum with a blackbody and calculate the effective wavelength of each channel,  $\lambda_{\text{eff}}$ , as follows:

$$\lambda_{\text{eff}} = \int_{\lambda_0 - \Delta\lambda/2}^{\lambda_0 + \Delta\lambda/2} F(\lambda) N(\lambda, T_e) \lambda d\lambda / \int_{\lambda_0 - \Delta\lambda/2}^{\lambda_0 + \Delta\lambda/2} F(\lambda) N(\lambda, T_e) d\lambda, \quad (4)$$

<sup>5</sup> As used in this paper, fringe visibility refers to fringe visibility amplitude—a real quantity.

where  $T_e$  is the effective stellar temperature estimated from the spectrum of each star (Allen 1983),  $\lambda_0$  and  $\Delta\lambda$  are the center wavelength and bandwidth of the filter,  $F(\lambda)$  is the quantum efficiency of the detector, and  $N(\lambda, T_e)$  is the blackbody photon distribution law.

### 2.3. Calibration of Measured Fringe Visibilities

A decrease in fringe visibility is inevitable because of imperfect optics, mechanical vibrations, and atmospheric turbulence. To calibrate this reduction, several reference stars, which have diameters less than or equal to 1 mas, are included in the observation list and are measured periodically. The normalization coefficient,  $NC$ , which is the ratio of the measured squared visibilities of the reference stars to their theoretical values, is calculated for all of the channels. A constant value of  $NC$  is used for each night. Typical values of  $NC$  are 0.77, 0.59, and 0.30 for the channels at 800, 550, and 450 nm, respectively.

The estimated diameters of the reference stars for our data processing are the mean values calculated from a number of observations made using the 32 m baseline. Fringe visibility measurements at both 800 and 550 nm were used, along with the assumption of a wavelength-independent diameter, to simultaneously estimate the normalization coefficient and the reference stars' diameters.

Given the diameters of the reference stars, the normalization coefficients for each night were calculated from the measured squared visibilities of these stars. The weights used in determining the normalization coefficients were  $1/\sigma_{\text{scan}}^2$ , as calculated above. The measurement error of the normalization coefficient for each night,  $\sigma_{NC}$ , is estimated as the rms of the individual  $NC$  measurements. The existence of systematic changes or trends of the normalization coefficients from different reference stars is carefully checked for each night.

### 2.4. Model Fitting of Fringe Visibility and Orbit Determination

The fringe visibility of a binary star as a function of time will vary periodically, depending on the baseline, the relative motion of the system, and the brightness ratio of the components. Taking advantage of the automatic operation of the Mark III Interferometer, sufficient data points for each binary can be gathered in a night to yield accurate model fits. Assuming that the changes in the relative position of the binary system in less than 10 hr are negligible, the separation and position angle of the binary system can be determined directly from the calibrated squared fringe visibilities.

The squared fringe visibility of a binary star,  $V^2$ , as a function of projected baseline  $d$ , is given by (cf. Hanbury Brown 1974)

$$V^2(d) = \frac{\Gamma_1^2(d) + [\gamma R \Gamma_2(d)]^2 + 2\gamma R \Gamma_1(d) \Gamma_2(d) \cos(2\pi d \rho \cos \psi / \lambda_{\text{eff}})}{(1 + R)^2}, \quad (5)$$

$$\Gamma_i(d) = \frac{2J_1(\pi d \theta_i'' / \lambda_{\text{eff}})}{\pi d \theta_i'' / \lambda_{\text{eff}}} \quad (i = 1, 2), \quad (6)$$

$$\gamma = \frac{\sin[\pi(\Delta\lambda/\lambda_{\text{eff}})d \rho \cos \psi / \lambda_{\text{eff}}]}{\pi(\Delta\lambda/\lambda_{\text{eff}})d \rho \cos \psi / \lambda_{\text{eff}}}. \quad (7)$$

In these expressions  $R$  is the intensity ratio of two components ( $R < 1$ );  $\theta_1''$  and  $\theta_2''$  are the angular diameters (equivalent

uniform disks) of the primary and the companion;  $\rho$  is the total angular separation of two components;  $\psi$  is the angle in the  $u$ - $v$  plane between the projection of the line connecting the components and the baseline; and  $\lambda_{\text{eff}}$  is the effective wavelength of the spectral channel. The factor  $\gamma$  accounts for the reduction of fringe visibility due to finite filter bandwidth and is given for a rectangular bandpass of width  $\Delta\lambda$ .

A nonlinear model-fitting algorithm (Levenberg-Marquardt) was developed to determine the intensity ratio, the separations of the components in right ascension and declination, and their formal errors for each night. The assumed sizes of the equivalent uniform circular disks of the components come from theoretical estimates and are discussed in detail later.

As a final step, the technique of differential correction is applied to compute the elements of the visual orbit (Heintz 1978). The formal errors for  $a''$ ,  $i$ ,  $\omega$ , and  $\Omega$  are calculated using standard Monte-Carlo methods; the formal errors for  $P$ ,  $T$ , and  $e$  are calculated directly from the formal errors of the nonlinear model fitting.

### 3. OBSERVATIONS AND ANALYSIS OF $\alpha$ ANDROMEDAE

The object  $\alpha$  And (HD 358, HR 15; R.A. =  $0^{\text{h}}08^{\text{m}}4$ , decl. =  $29^{\circ}05'4$  for equinox 2000.0) is a single-line spectroscopic binary and is also the bright component of ADS 94; the companion is  $11^{\text{m}}4$  at  $75''$ . This binary system has a total visual magnitude  $m_v = 2.06$  mag and has been classified as spectral type B8, B8.5 (Petrie 1950), A0 (Eggen 1957), B9 III (Johnson et al. 1966), and more recently, as B8 IV by Hoffleit & Jaschek (1982) and Derman (1982). The far-ultraviolet line spectrum of  $\alpha$  And is more similar to spectral types B3–B6, luminosity classes III–V (Aydin & Hack 1978).  $\alpha$  And is a chemically peculiar star and belongs to the subclassification of mercury-manganese stars. Many investigations on its effective temperature, radii, atmospheric model, and evolutionary behavior (Adelman 1983; Babu 1977; Shallis & Blackwell 1979; Eggen 1972; Jugaku & Sargent 1968) have been conducted. Evidence has been found of light variations at UV wavelengths with a period of  $0^{\text{d}}96$  and an amplitude of 0.06 mag and of velocity variations of up to  $10 \text{ km s}^{-1}$  with a period of about  $0^{\text{d}}13$  (Rakos, Jenker, & Wood 1981).

The object  $\alpha$  And has a long history of spectroscopic observations starting with Baker (1908) and Ludendorff (1908). More recent results were reported by Pearce (1936), Kohl

(1937), Luyten, Struve, & Morgan (1939), Abt & Snowden (1973), and Aikman (1976). The orbital elements determined by different authors are consistent within their given precision. The quality of the orbit determination of this system from spectroscopy is judged to be of class "b" in the Eighth Catalogue of the Orbital Elements of Spectroscopic Binary Systems (Batten, Fletcher, & McCarthy 1989). This means that the elements are determined with better than average precision, but cannot be considered definitive. The spectroscopic results are listed in Table 6. McAlister & Hartkopf (1988) observed this system with speckle interferometry and concluded that the separation was less than 30 mas.

Observations of  $\alpha$  And with the Mark III Stellar Interferometer began in 1988. Using the data from 1988, predictions of the relative positions for 1989 were made, and longer baselines and more scans per night were scheduled for that year. The reference stars were carefully selected and were uniformly distributed throughout the nights. A total of 22 nights of good observations, nine in 1988 and 13 in 1989, on 12 different baselines were obtained for the 800 nm channel; 20 of these nights had good data on the 550 nm channel.

Table 1 lists the mean normalization coefficients and their rms fluctuations throughout the night determined from reference stars and applied to the observations of  $\alpha$  And in 1989. These normalization coefficients at 800 nm and 550 nm vary from night to night by up to  $\sim 0.12$ , depending on the instrument alignment and configuration, and on the seeing. The rms measurement errors also vary from 0.02 to 0.06 among nights, depending on the seeing conditions. Typical plots of the normalization coefficients of the reference stars at 800 nm and 550 nm as a function of time are given in Figures 1a–1b and exhibit mostly random fluctuations throughout the night. The values of the normalization coefficients for different reference stars on that night are given in Table 2. The estimated range of diameters for the reference stars is from 0.3 to 1 mas. If a 0.3 mas star were mistakenly estimated as 1 mas, it would introduce systematic errors of up to 0.07 at 800 nm and 0.12 at 550 nm at the longest baseline. However, the typical rms fluctuations of the normalization coefficients for different reference stars are less than 0.025. The corresponding uncertainty of the diameter of a 1 mas reference star is less than  $\sim 0.15$  mas; the nightly calibration precisions are  $\sim 1\%$  at 800 nm and  $\sim 2\%$  at 550 nm.

TABLE 1  
MEAN NORMALIZATION COEFFICIENTS (NC) AND RMS FLUCTUATIONS THROUGHOUT THE NIGHT FOR  
OBSERVATIONS OF  $\alpha$  ANDROMEDAE IN 1989

DATE (1989)	800 nm		550 nm		NUMBER OF SCANS	NUMBER OF STARS	BASELINE (m)
	NC	rms	NC	rms			
Aug 13 .....	0.781	0.028	0.581	0.028	19	3	11.4
Aug 16 .....	0.706	0.043	0.529	0.042	25	3	15.1
Aug 27 .....	0.804	0.033	0.608	0.020	10	1	26.9
Aug 31 .....	0.773	0.031	0.571	0.021	39	2	31.4
Sep 2 .....	0.756	0.023	0.558	0.022	15	2	31.4
Sep 3 .....	0.723	0.026	0.508	0.030	56	5	31.4
Sep 5 .....	0.822	0.025	0.632	0.030	11	2	27.5
Sep 6 .....	0.768	0.054	0.601	0.039	32	2	27.5
Sep 8 .....	0.767	0.052	0.599	0.053	31	3	23.5
Sep 9 .....	0.802	0.034	0.625	0.049	39	3	23.5
Sep 14 .....	0.782	0.057	0.596	0.061	48	4	8.1
Oct 6 .....	0.821	0.044	0.644	0.030	41	4	31.4
Oct 7 .....	0.777	0.062	0.582	0.058	46	6	31.4

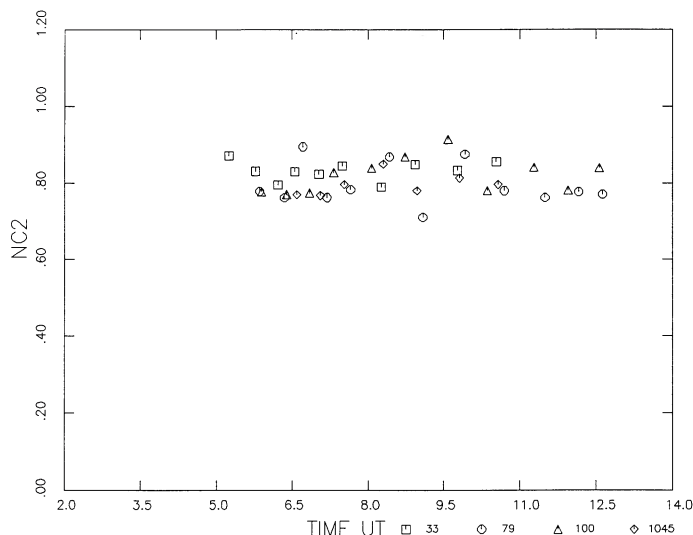


FIG. 1a

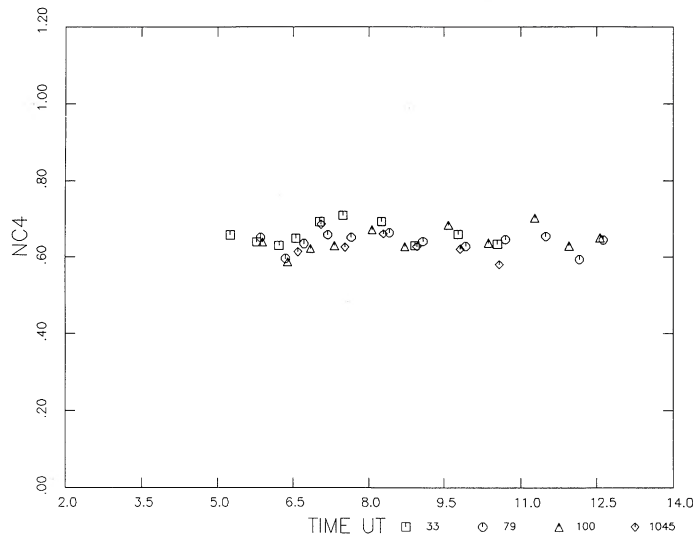


FIG. 1b

FIG. 1.—(a) Normalization coefficients of reference stars vs. time at 800 nm on baseline 38 (31.4 m), 1989 October 6. The rms fluctuations of the normalization coefficients is  $\pm 0.044$ . The rms fluctuations of normalization coefficients from different reference stars is  $\pm 0.018$ . (b) Normalization coefficients of reference stars vs. time at 550 nm on baseline 38 (31.4 m), 1989 October 6. The rms fluctuations of the normalization coefficients is  $\pm 0.030$ . The rms fluctuation of normalization coefficients from different reference stars is  $\pm 0.012$ .

Two sources of error in the calibrated squared visibility ( $V^2$ ) for the program stars are considered: measurement error of the raw squared visibility ( $V_{\text{raw}}^2$ ) and calibration error. The total error,  $\sigma_{V^2}^2$ , of each calibrated scan is estimated as

$$\sigma_{V^2}^2 = \sigma_{\text{scan}}^2 / NC^2 + (V_{\text{raw}}^2)^2 \sigma_{NC}^2 / NC^4, \quad (8)$$

where  $\sigma_{\text{scan}}$  is the measurement error of  $V_{\text{raw}}^2$  for the scan, and  $NC$  and  $\sigma_{NC}$  are the normalization coefficient and its measurement error, respectively.

Model fitting to the calibrated squared visibilities was carried out to determine the angular separations in the directions of right ascension and declination on the sky,  $S_r$  and  $S_d$ . Tables 3A and 3B give the results with their formal ( $1\sigma$ ) errors. In addition, the tables include the error of fit to the calibrated squared visibilities. The assumed diameters of the two components are 1.1 and 0.5 mas, as discussed in the last section. Model-fitting errors (rms) are generally less than 0.05 in  $V^2$  and are consistent with the measurement errors used in calculating  $\chi^2$ . Typical examples of measured and best-fit squared fringe visibilities as a function of time are shown in Figures 2a–2d and 3a–3d for 800 and 550 nm, respectively.

#### 4. ORBITAL MOTION AND MAGNITUDE DIFFERENCE OF $\alpha$ ANDROMEDAE

##### 4.1. Orbital Motion

The binary system  $\alpha$  And was first resolved with the Mark III Stellar Interferometer in 1988. At that time, its visual orbit was determined by adopting two parameters, period  $P$  and epoch  $T$ , from spectroscopy, yielding the results given in columns (2) and (3) of Table 4. Predictions of its relative positions were made for 1989 and are compared with measurements for 1989 August 31 in Table 5. For this example, an accuracy of 0.1 mas was obtained for predictions of the relative positions of the binary.

Table 4 gives the eccentricity and geometric elements for different time periods assuming period  $P = 96^d.696$  and epoch  $T = \text{JD } 2,447,374.60$ . The excellent consistency of the above results reflects the high accuracy of fringe visibility measurements with the Mark III Interferometer. In fact, only nine measurements in 1988 covering  $159^\circ$  of mean anomaly, or 44% of a revolution, have already provided a good determination of the visual orbit.

TABLE 2  
NORMALIZATION COEFFICIENTS AND rms FLUCTUATIONS FOR DIFFERENT REFERENCE STARS ON  
1989 OCTOBER 6

STAR (FK5)	NAME	ESTIMATED DIAMETER (mas)	800 nm		550 nm		NUMBER OF SCANS
			NC	rms	NC	rms	
33	$\mu$ And	0.50	0.840	0.025	0.658	0.028	10
79	$\gamma$ Tri	0.48	0.816	0.055	0.642	0.024	12
100	HR838	0.46	0.818	0.055	0.640	0.031	12
1045	$\nu$ And	0.84	0.796	0.029	0.630	0.034	7
$\overline{NC}$			0.820		0.643		
rms			0.018		0.012		

TABLE 3  
ESTIMATED ANGULAR SEPARATIONS WITH FORMAL ( $1\sigma$ ) ERRORS AND rms MODEL-FITTING  
ERRORS ( $\epsilon$ ) TO CALIBRATED  $V^2$  FOR  $\alpha$  ANDROMEDAE

Epoch JD 2,400,000+	$S_r$ (mas)	$S_d$ (mas)	Scans	$\epsilon$ ( $V^2$ )	Baseline (m)
A. 800 nm					
47412.9215.....	$-17.76 \pm 0.21$	$-4.19 \pm 0.14$	17	0.023	11.9
47413.8603.....	$-16.93 \pm 0.54$	$-4.60 \pm 0.16$	10	0.015	11.9
47436.7827.....	$2.41 \pm 0.72$	$-10.39 \pm 0.30$	20	0.014	11.4
47437.8351.....	$2.61 \pm 0.78$	$-9.72 \pm 0.62$	20	0.030	19.0
47438.7458.....	$3.36 \pm 0.64$	$-9.99 \pm 0.12$	29	0.027	19.0
47457.7650.....	$15.93 \pm 0.21$	$-7.91 \pm 0.05$	20	0.030	23.0
47458.7741.....	$16.58 \pm 0.13$	$-7.35 \pm 0.04$	13	0.015	27.5
47459.8278.....	$16.36 \pm 0.32$	$-6.90 \pm 0.12$	11	0.018	31.4
47460.8263.....	$16.56 \pm 0.13$	$-6.33 \pm 0.04$	16	0.023	31.4
47751.8909.....	$16.04 \pm 0.60$	$-5.66 \pm 0.14$	13	0.018	11.4
47754.8830.....	$14.60 \pm 0.59$	$-3.43 \pm 0.17$	12	0.039	15.1
47765.9028.....	$-8.60 \pm 0.23$	$4.85 \pm 0.05$	21	0.016	26.9
47769.8954.....	$-15.94 \pm 0.11$	$5.17 \pm 0.03$	34	0.020	31.4
47771.8734.....	$-18.59 \pm 0.10$	$4.95 \pm 0.03$	19	0.016	31.4
47772.8278.....	$-19.39 \pm 0.25$	$4.70 \pm 0.07$	12	0.034	31.4
47774.8952.....	$-21.11 \pm 0.19$	$4.25 \pm 0.05$	14	0.016	27.5
47775.8808.....	$-21.75 \pm 0.38$	$4.01 \pm 0.11$	26	0.035	27.5
47777.9070.....	$-22.85 \pm 0.59$	$3.31 \pm 0.16$	16	0.054	23.5
47778.8882.....	$-23.15 \pm 0.19$	$3.05 \pm 0.06$	22	0.023	23.5
47783.8773.....	$-22.43 \pm 1.09$	$1.17 \pm 0.32$	16	0.030	8.1
47805.8012.....	$-13.46 \pm 0.38$	$-6.29 \pm 0.08$	11	0.025	31.4
47806.7684.....	$-12.19 \pm 0.74$	$-6.75 \pm 0.19$	12	0.044	31.4
B. 550 nm					
47412.9215.....	$17.83 \pm 0.44$	$-4.17 \pm 0.31$	17	0.043	11.9
47413.8603.....	$-17.64 \pm 0.67$	$-4.81 \pm 0.22$	10	0.052	11.9
47437.8351.....	$2.57 \pm 0.28$	$-10.20 \pm 0.13$	20	0.026	19.0
47438.7458.....	$3.49 \pm 0.16$	$-10.65 \pm 0.07$	29	0.043	19.0
47457.7650.....	$15.63 \pm 0.39$	$-7.86 \pm 0.09$	20	0.070	23.0
47458.7741.....	$16.44 \pm 0.17$	$-7.32 \pm 0.05$	13	0.039	27.5
47459.8278.....	$16.79 \pm 0.77$	$-6.85 \pm 0.32$	11	0.069	31.4
47460.8263.....	$16.68 \pm 0.19$	$-6.30 \pm 0.06$	16	0.043	31.4
47751.8909.....	$16.50 \pm 0.67$	$-5.84 \pm 0.20$	13	0.028	11.4
47754.8830.....	$15.40 \pm 0.78$	$-3.48 \pm 0.22$	12	0.029	15.1
47765.9028.....	$-8.57 \pm 0.15$	$4.80 \pm 0.04$	21	0.025	26.9
47769.8954.....	$-15.90 \pm 0.10$	$5.19 \pm 0.03$	34	0.030	31.4
47771.8734.....	$-18.62 \pm 0.12$	$4.95 \pm 0.04$	19	0.025	31.4
47772.8278.....	$-19.46 \pm 0.26$	$4.69 \pm 0.08$	12	0.049	31.4
47774.8952.....	$-21.28 \pm 0.21$	$4.29 \pm 0.07$	14	0.022	27.5
47775.8808.....	$-21.88 \pm 0.24$	$3.98 \pm 0.08$	26	0.035	27.5
47777.9070.....	$-22.64 \pm 0.48$	$32.5 \pm 0.15$	16	0.049	23.5
47778.8882.....	$-23.06 \pm 0.29$	$3.06 \pm 0.10$	22	0.051	23.5
47783.8773.....	$-22.41 \pm 1.59$	$0.72 \pm 0.55$	16	0.046	8.1
47806.7684.....	$-11.70 \pm 0.85$	$-6.64 \pm 0.13$	12	0.119	31.4

TABLE 4  
ORBITAL ELEMENTS OF  $\alpha$  ANDROMEDAE FOR DIFFERENT TIME INTERVALS ASSUMING PERIOD  $P = 96^d696$ , EPOCH  $T = \text{JD } 2,447,374.60$

PARAMETER (1)	1988		1989		1988 AND 1989	
	800 nm (2)	550 nm (3)	800 nm (4)	550 nm (5)	800 nm (6)	550 nm (7)
$e$ .....	$0.529 \pm 0.009$	$0.516 \pm 0.020$	$0.529 \pm 0.009$	$0.526 \pm 0.012$	$0.534 \pm 0.002$	$0.531 \pm 0.003$
$a''$ (mas).....	$24.12 \pm 0.21$	$24.06 \pm 0.39$	$24.16 \pm 0.22$	$24.16 \pm 0.23$	$24.14 \pm 0.15$	$24.14 \pm 0.29$
$i$ (degrees).....	$105.52 \pm 0.32$	$106.26 \pm 0.56$	$105.57 \pm 0.50$	$105.44 \pm 0.52$	$105.69 \pm 0.25$	$105.98 \pm 0.46$
$w$ (degrees).....	$77.13 \pm 0.36$	$77.36 \pm 0.68$	$77.46 \pm 0.64$	$77.93 \pm 1.34$	$77.18 \pm 0.38$	$77.41 \pm 0.57$
$\Omega$ (degrees).....	$104.57 \pm 0.44$	$104.14 \pm 0.87$	$104.28 \pm 0.30$	$104.41 \pm 0.46$	$104.30 \pm 0.36$	$104.26 \pm 0.36$

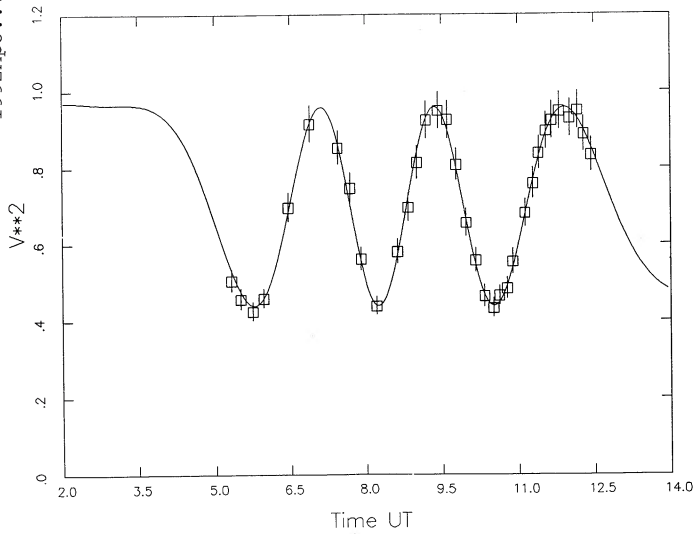


FIG. 2a

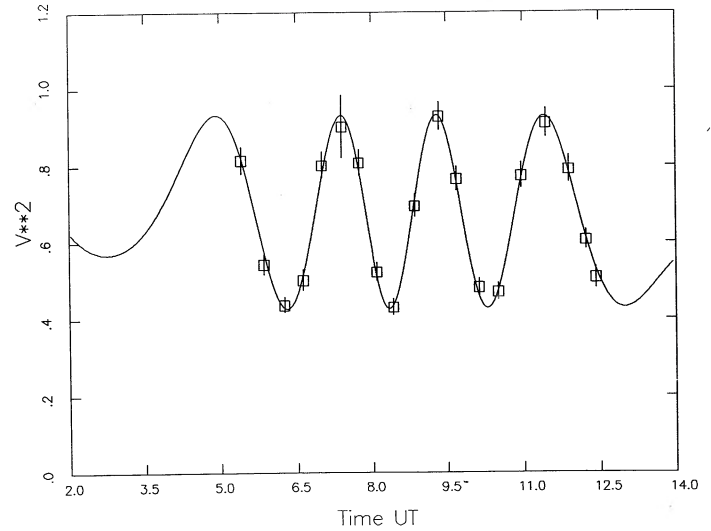


FIG. 2b

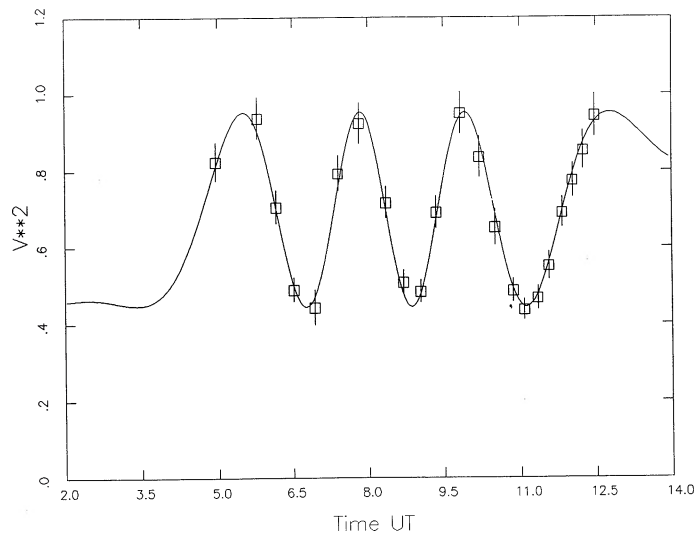


FIG. 2c

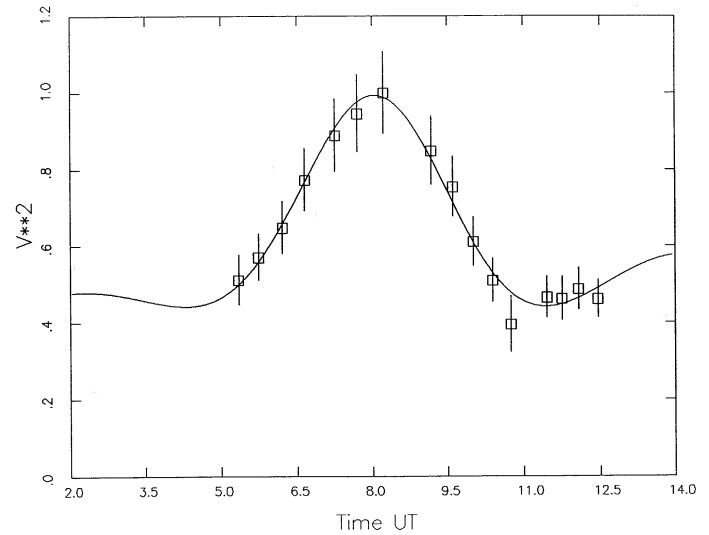


FIG. 2d

FIG. 2.—(a) Measured and best-fit fringe visibilities for  $\alpha$  And at 800 nm on baseline 38 (31.4 m), 1989 August 31. The errors of each individual scan ( $\pm 1 \sigma$ ) are indicated by vertical lines around the measured data. The best-fit curve corresponds to intensity ratio  $R = 0.191$ , and separations in R.A. and decl. of  $-15.94$  mas and  $5.17$  mas, respectively. The rms error of fit to the calibrated squared visibilities ( $V^2$ ) is  $0.02$ . (b) Measured and best-fit fringe visibilities for  $\alpha$  And at 800 nm on baseline 38 (31.4 m), 1989 September 2. The errors of each individual scan ( $\pm 1 \sigma$ ) are indicated by vertical lines around the measured data. The best-fit curve corresponds to intensity ratio  $R = 0.187$ , and separations in R.A. and decl. of  $-18.59$  mas and  $4.95$  mas, respectively. The rms error of fit to the calibrated squared visibilities ( $V^2$ ) is  $0.016$ . (c) Measured and best-fit fringe visibilities for  $\alpha$  And at 800 nm on baseline 33 (23.5 m), 1989 September 9. The errors of each individual scan ( $\pm 1 \sigma$ ) are indicated by vertical lines around the measured data. The best-fit curve corresponds to intensity ratio  $R = 0.185$ , and separations in R.A. and decl. of  $-23.15$  mas and  $3.05$  mas, respectively. The rms error of fit to the calibrated squared visibilities ( $V^2$ ) is  $0.023$ . (d) Measured and best-fit fringe visibilities for  $\alpha$  And at 800 nm on baseline 9 (8.1 m), 1989 September 14. The errors of each individual scan ( $\pm 1 \sigma$ ) are indicated by vertical lines around the measured data. The best-fit curve corresponds to intensity ratio  $R = 0.199$ , and separations in R.A. and decl. of  $-22.43$  mas and  $1.17$  mas, respectively. The rms error of fit to the calibrated squared visibilities ( $V^2$ ) is  $0.030$ .

While the results in Table 4 make use of orbital parameters from spectroscopy, the total observations of  $\alpha$  And with the Mark III Interferometer in 1988 and 1989 cover more than four revolutions of its orbital motion, and thus all seven orbital elements can be determined independently of spectroscopic data, and are given in Table 6. Also included in Table 6 are the spectroscopic results. The orbital elements from these two completely different techniques are in very good agreement.

However, the three orbital parameters,  $a''$ ,  $i$ ,  $\Omega$ , can only be determined from the interferometric data. The combined results listed in the last column of Table 6 are the weighted average values from interferometric and spectroscopic observations.

The observed ( $O$ ) and calculated ( $C$ ) separations  $S$ , and  $S_d$ , the residuals to the visual orbit ( $O - C$ ), the corresponding total separation  $\rho''$ , and the mean anomaly  $E$ , are presented in

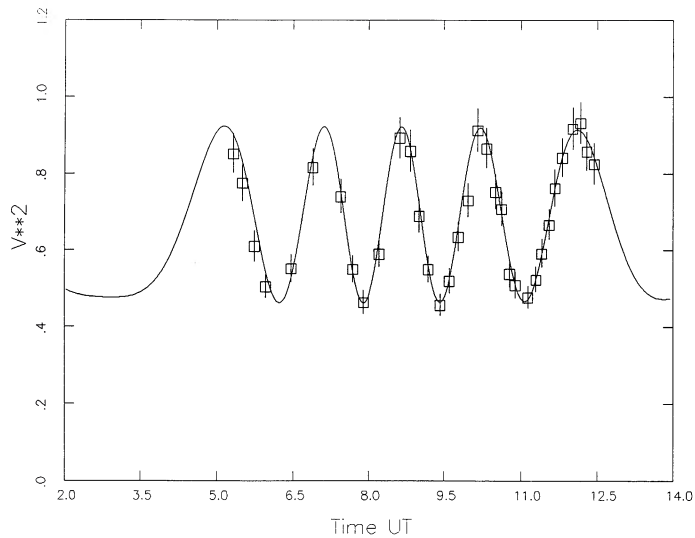


FIG. 3a

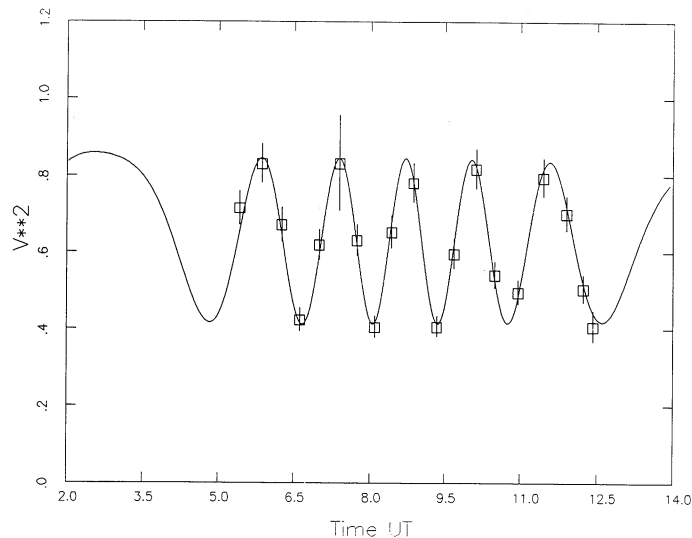


FIG. 3b

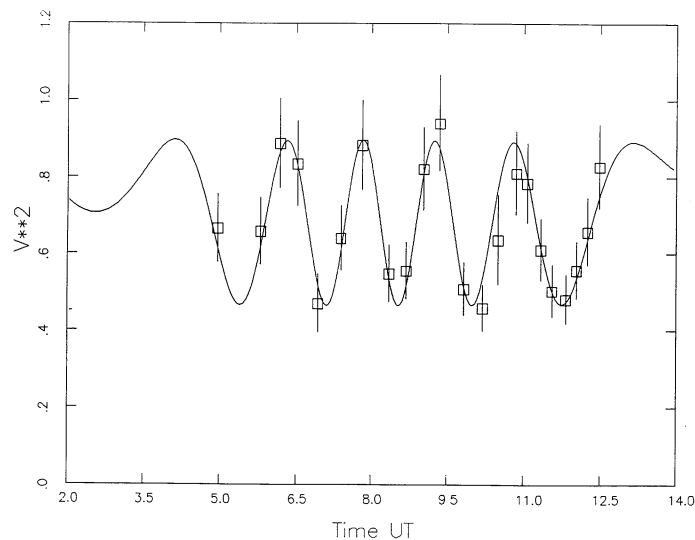


FIG. 3c

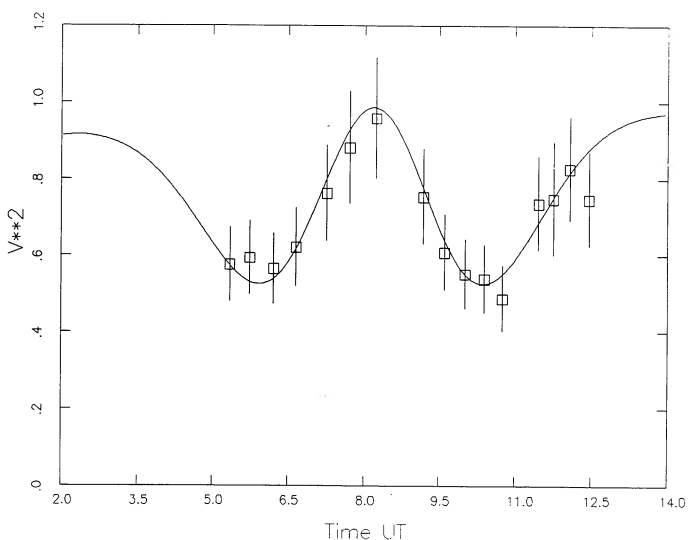


FIG. 3d

FIG. 3.—(a) Measured and best-fit fringe visibilities for  $\alpha$  And at 550 nm on baseline 38 (31.4 m), 1989 August 31. The errors of each individual scan ( $\pm 1 \sigma$ ) are indicated by vertical lines around the measured data. The best-fit curve corresponds to intensity ratio  $R = 0.158$ , and separations in R.A. and decl. of  $-15.90$  mas and  $5.19$  mas, respectively. The rms error of fit to the calibrated squared visibilities ( $V^2$ ) is  $0.030$ . (b) Measured and best-fit fringe visibilities for  $\alpha$  And at 550 nm on baseline 38 (31.4 m), 1989 September 2. The errors of each individual scan ( $\pm 1 \sigma$ ) are indicated by vertical lines around the measured data. The best-fit curve corresponds to intensity ratio  $R = 0.166$ , and separations in R.A. and decl. of  $-18.62$  mas and  $4.95$  mas, respectively. The rms error of fit to the calibrated squared visibilities ( $V^2$ ) is  $0.025$ . (c) Measured and best-fit fringe visibilities for  $\alpha$  And at 550 nm on baseline 33 (23.5 m), 1989 September 9. The errors of each individual scan ( $\pm 1 \sigma$ ) are indicated by vertical lines around the measured data. The best-fit curve corresponds to intensity ratio  $R = 0.154$ , and separations in R.A. and decl. of  $-23.06$  mas and  $3.06$  mas, respectively. The rms error of fit to the calibrated squared visibilities ( $V^2$ ) is  $0.051$ . (d) Measured and best-fit fringe visibilities for  $\alpha$  And at 550 nm on baseline 9 (8.1 m), 1989 September 14. The errors of each individual scan ( $\pm 1 \sigma$ ) are indicated by vertical lines around the measured data. The best-fit curve corresponds to intensity ratio  $R = 0.155$ , and separations in R.A. and decl. of  $-22.41$  mas and  $0.72$  mas, respectively. The rms error of fit to the calibrated squared visibilities ( $V^2$ ) is  $0.046$ .

Tables 7A and 7B for wavelengths of 800 and 550 nm, respectively. The visual orbit of  $\alpha$  And and the measured data at 800 nm are plotted in Figure 4. The individual data points, which are at the center of the open circles, are connected to the calculated positions by a short line. The formal error is indicated by the lengths of the crosses centered on each point. One measurement in the figure is seen to have errors greater than 1 mas. This measurement was made with an 8.1 m projected baseline, whose resolution proved to be insufficient for the separation

between the two components (less than 24 mas) on that night. Because of the shortness of the baseline and the orientation of the binary, it took 6 hr to cover just one cycle of fringe visibility fluctuations (see Figs. 2d and 3d). With the longer baselines, many more cycles of visibility fluctuations occur during the night, yielding much better accuracy. Excluding that night's data, the mean residuals ( $O-C$ ) in Tables 7A and 7B are  $-0.05$  and  $0.01$  mas at 800 nm, and  $-0.02$  and  $0.02$  mas at 550 nm in the directions of right ascension and declination, respec-

TABLE 5  
PREDICTED AND MEASURED ORBITAL POSITIONS OF  
 $\alpha$  ANDROMEDAE ON 1989 AUGUST 31

Separation	Predicted (mas)	Measured at 800 nm (mas)	Measured at 550 nm (mas)
$S_r$ .....	-15.91	$-15.94 \pm 0.11$	$-15.90 \pm 0.10$
$S_d$ .....	5.26	$5.17 \pm 0.03$	$5.19 \pm 0.03$

tively. The rms dispersions of the observations from the orbit are  $\pm 0.23$  and  $\pm 0.14$  mas at 800 nm, and  $\pm 0.39$  and  $\pm 0.17$  mas at 550 nm in the two directions. These submilliarcsecond dispersions are of the same order as the average uncertainties of the separations,  $S_r$  and  $S_d$ , given in Tables 3A and 3B.

#### 4.2. Magnitude Difference

It is extremely difficult to measure the brightness difference between the two components of a spectroscopic binary because of the small angular separation. However, interferometric techniques can provide an accurate determination of the magnitude difference.

The determination of the magnitude difference between the components of  $\alpha$  And was done in two steps. Initially, the diameters of the components were assumed to be 1 mas. With this assumption, an estimated magnitude difference was determined by fitting to all of the observations for each night. Using this preliminary magnitude difference at 550 nm, as discussed in next section, the spectrum of the companion and the distance and masses of the individual components were estimated. Next, by using better estimated diameters of the two components, the magnitude difference was recalculated for each night; the resultant changes in magnitude difference were small compared with the error bars. The final results for the magnitude difference are the weighted averages for all observations.

The results for the magnitude difference of  $\alpha$  And at 800 and 550 nm, determined from 12 nights in 1989, are listed in Table 8. The average intensity ratios are  $0.188 \pm 0.006$  at 800 nm and  $0.160 \pm 0.005$  at 550 nm, and the corresponding magnitude differences are  $1.82 \pm 0.04$  mag and  $1.99 \pm 0.04$  mag (for this measurement, we conservatively estimate the formal error as the rms of the values from the individual nights). Given a total visual magnitude  $m_v = 2.06$  mag, the visual magnitudes of the primary and the companion are determined as  $2.22 \pm 0.01$  mag and  $4.21 \pm 0.04$  mag, respectively. Utilizing the multicolor photometric observations  $V-R = -0.03$  mag and  $V-I = -0.13$  mag (Johnson et al. 1966),  $V-800$  nm is esti-

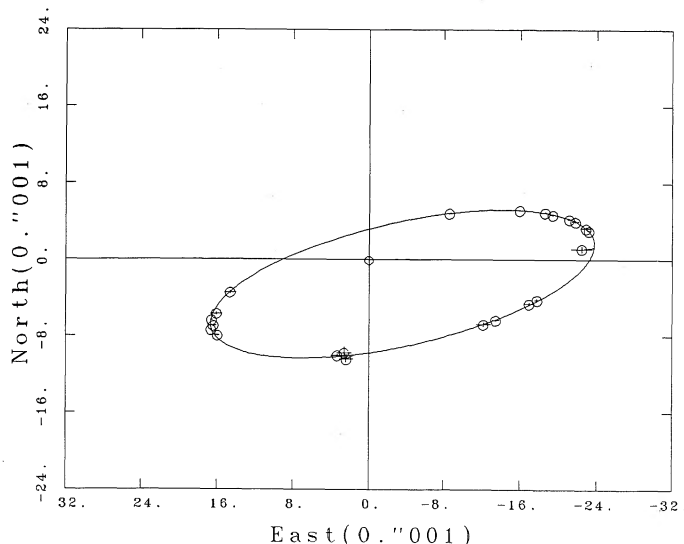


FIG. 4.—Measured data at 800 nm and apparent orbit of  $\alpha$  And. The individual measurements, which are at the centers of the open circles, are connected to the calculated positions by a short line. The formal errors ( $\pm 1 \sigma$ ) in R.A. and decl. are indicated by the lengths of crosses centered on the points.

mated as  $-0.08 \pm 0.02$  mag, and the magnitude of the two components of  $\alpha$  And at 800 nm are calculated as  $2.33 \pm 0.02$  mag and  $4.15 \pm 0.04$  mag, respectively. Thus, the color indices of the primary and the companion between 550 and 800 nm are determined as  $-0.11 \pm 0.03$  mag and  $+0.07 \pm 0.05$  mag. These results indicate that the blue primary and the white companion correspond to a late-type B star and an early-type A star.

It is interesting to note that Petrie determined  $\Delta m = 1.35$  mag from spectrophotometric measurements (Petrie 1950). But this is certainly an underestimate (Derman 1982). As Derman remarked, Petrie identified the line  $\lambda 4479$  Mn II of the primary spectrum as the secondary component of  $\lambda 4481$  Mg II on at least some of his tracings.

#### 5. DISCUSSION

All seven orbital parameters of  $\alpha$  And have been determined accurately with the Mark III Interferometer and agree well with the spectroscopic results. With the combined results from interferometry and spectroscopy, one can determine the astrophysical properties of a star. Although  $\alpha$  And is a single-line spectroscopic binary and has not had a direct measurement of the linear size of the companion's orbit from spectroscopy, the

TABLE 6  
COMPARISON BETWEEN THE MARK III INTERFEROMETER AND SPECTROSCOPY FOR THE ORBITAL ELEMENTS OF  $\alpha$  ANDROMEDAE  
( $1 \sigma$  FORMAL ERRORS)

$\alpha$ ANDROMEDAE	MARK III		SPECTROSCOPY (Aikman 1976)	COMBINED
	800 nm	550 nm		
$P$ (days) .....	$96.627 \pm 0.101$	$96.689 \pm 0.103$	$96.6960 \pm 0.0013$	$96.6960 \pm 0.0013$
$T$ (JD) .....	$2,447,374.84 \pm 0.24$	$2,447,374.85 \pm 0.29$	$2,442,056.32 \pm 0.28$	$2,447,374.77 \pm 0.15$
$e$ .....	$0.529 \pm 0.006$	$0.530 \pm 0.010$	$0.521 \pm 0.008$	$0.527 \pm 0.004$
$a''$ (mas) .....	$24.09 \pm 0.15$	$24.37 \pm 0.29$	...	$24.15 \pm 0.13$
$i$ (degrees) .....	$105.62 \pm 0.25$	$105.79 \pm 0.46$	...	$105.66 \pm 0.22$
$w$ (degrees) .....	$77.24 \pm 0.38$	$77.46 \pm 0.57$	$77.1 \pm 1.3$	$77.31 \pm 0.32$
$\Omega$ (degrees) .....	$104.27 \pm 0.36$	$104.04 \pm 0.36$	...	$104.16 \pm 0.25$



TABLE 7  
ORBIT RESIDUALS FOR  $\alpha$  ANDROMEDAE

Epoch JD 2,400,000 +	$S_1(O)$ (mas)	$S_1(C)$ (mas)	$(O-C)_1$ (mas)	$S_2(O)$ (mas)	$S_2(C)$ (mas)	$(O-C)_2$ (mas)	$\rho$ (mas)	$E$
A. 800 nm								
47412.9215.....	-17.76	-17.41	-0.35	-4.19	-4.34	0.15	17.95	154.79
47413.8603.....	-16.93	-16.81	-0.12	-4.60	-4.65	0.05	17.44	157.15
47436.7827.....	2.41	1.69	0.72	-10.39	-9.95	-0.44	10.09	213.88
47437.8351.....	2.61	2.61	0.00	-9.72	-10.06	0.34	10.39	216.62
47438.7458.....	3.36	3.40	-0.04	-9.99	-10.13	0.14	10.69	219.01
47457.7650.....	15.93	16.27	-0.34	-7.91	-7.80	-0.11	18.04	279.02
47458.7741.....	16.58	16.47	0.11	-7.35	-7.37	0.02	18.04	283.20
47459.8278.....	16.36	16.57	-0.21	-6.90	-6.87	-0.03	17.93	287.77
47460.8263.....	16.56	16.54	0.02	-6.33	-6.34	0.01	17.71	292.32
47751.8909.....	16.04	16.33	-0.29	-5.66	-5.65	-0.01	17.28	298.01
47754.8830.....	14.60	14.67	-0.07	-3.43	-3.55	0.12	15.09	314.18
47765.9028.....	-8.60	-8.58	-0.02	4.85	4.84	0.01	9.85	33.85
47769.8954.....	-15.94	-15.88	-0.06	5.17	5.17	0.00	16.70	57.37
47771.8734.....	-18.59	-18.36	-0.23	4.95	4.92	0.03	19.01	67.14
47772.8278.....	-19.39	-19.34	-0.05	4.70	4.74	-0.04	19.91	71.52
47774.8952.....	-21.11	-21.02	-0.09	4.25	4.24	0.01	21.44	80.35
47775.8808.....	-21.75	-21.64	-0.11	4.01	3.97	0.04	22.00	84.30
47777.9070.....	-22.85	-22.60	-0.25	3.31	3.35	-0.04	22.84	91.98
47778.8882.....	-23.15	-22.92	-0.23	3.05	3.03	0.02	23.12	95.52
47783.8773.....	-22.43	-22.44	1.01	1.17	1.27	-0.10	23.48	112.03
47805.8012.....	-13.46	-12.98	-0.48	-6.29	-6.33	0.04	14.44	170.58
47806.7684.....	-12.19	-12.25	0.06	-6.75	-6.60	-0.15	13.91	172.94
B. 550 nm								
47412.9215.....	-17.83	-17.62	-0.21	-4.17	-4.56	0.39	18.20	154.72
47413.8603.....	-17.64	-17.02	-0.62	-4.81	-4.87	0.06	17.70	157.08
47437.8351.....	2.57	2.45	0.12	-10.20	-10.22	0.02	10.50	216.47
47438.7458.....	3.49	3.24	0.25	-10.65	-10.29	-0.36	10.79	218.86
47457.7650.....	15.63	16.27	-0.64	-7.86	-7.84	-0.02	18.06	278.71
47458.7741.....	16.44	16.48	-0.04	-7.32	-7.40	0.08	18.07	282.88
47459.8278.....	16.79	16.59	0.20	-6.85	-6.90	0.05	17.97	287.43
47460.8263.....	16.68	16.58	0.10	-6.30	-6.36	0.06	17.76	291.96
47751.8909.....	16.50	16.43	0.07	-5.84	-5.78	-0.06	17.42	296.71
47754.8830.....	15.40	14.95	0.45	-3.48	-3.70	0.22	15.40	312.64
47765.9028.....	-8.57	-8.02	-0.55	4.80	4.78	0.02	9.34	32.18
47769.8954.....	-15.90	-15.57	-0.33	5.19	5.14	0.05	16.40	56.07
47771.8734.....	-18.62	-18.16	-0.46	4.95	4.89	0.06	18.81	65.97
47772.8278.....	-19.46	-19.18	-0.28	4.69	4.71	-0.02	19.75	70.40
47774.8952.....	-21.28	-20.95	-0.33	4.29	4.21	0.08	21.37	79.33
47775.8808.....	-21.88	-21.61	-0.27	3.98	3.93	0.05	21.96	83.32
47777.9070.....	-22.64	-22.63	-0.01	3.25	3.30	-0.05	22.87	91.06
47778.8882.....	-23.06	-22.98	-0.08	3.06	2.97	0.09	23.17	94.62
47783.8773.....	-22.41	-23.62	1.21	0.72	1.18	-0.46	23.65	111.23
47806.7684.....	-11.70	-12.64	0.94	-6.64	-6.75	0.11	14.33	172.25

TABLE 8  
INTENSITY RATIOS AND  $1\sigma$  FORMAL ERRORS FOR OBSERVATIONS OF  
 $\alpha$  ANDROMEDAE IN 1989

Date	800 nm	550 nm	Scans	Baseline (m)
Aug 13.....	0.184 $\pm$ 0.014	0.158 $\pm$ 0.012	13	11.4
Aug 16.....	0.183 $\pm$ 0.024	0.161 $\pm$ 0.030	12	15.1
Aug 27.....	0.196 $\pm$ 0.012	0.160 $\pm$ 0.012	21	26.9
Aug 31.....	0.191 $\pm$ 0.008	0.158 $\pm$ 0.009	34	31.4
Sep 2.....	0.187 $\pm$ 0.010	0.166 $\pm$ 0.012	19	31.4
Sep 3.....	0.183 $\pm$ 0.011	0.168 $\pm$ 0.020	12	31.4
Sep 5.....	0.190 $\pm$ 0.012	0.158 $\pm$ 0.021	14	27.5
Sep 6.....	0.190 $\pm$ 0.030	0.168 $\pm$ 0.024	26	27.5
Sep 8.....	0.179 $\pm$ 0.021	0.158 $\pm$ 0.034	16	23.5
Sep 9.....	0.185 $\pm$ 0.012	0.154 $\pm$ 0.026	22	23.5
Sep 14.....	0.199 $\pm$ 0.033	0.155 $\pm$ 0.041	16	8.1
Oct 6.....	0.189 $\pm$ 0.019	...	11	31.4
$\bar{R}$ .....	0.188 $\pm$ 0.006	0.160 $\pm$ 0.005	...	...
$\Delta m$ (mag).....	1.82 $\pm$ 0.04	1.99 $\pm$ 0.04	...	...

new results here do permit one to make a preliminary estimate of the mass ratio  $r = \mathcal{M}_2/\mathcal{M}_1 = a_1/a_2$ .

Given spectral type B8 IV for the primary component of  $\alpha$  And, and given a measured magnitude difference at visual wavelengths of  $\Delta m = 1.99$  mag, we estimate that the companion is most likely A3 V (Allen 1983). This estimate is consistent with the color indices determined above. From the mass-luminosity relation and the bolometric corrections of B8 IV and A3 V stars (Allen 1983; Smith 1983), the mass ratio is estimated as  $r \sim 0.48$ . Using the measured values of inclination  $i = 105^\circ.66$  and period  $P = 96^d.696$ , the linear semimajor axis  $a_1 \sin i = 34.2 \times 10^6$  km (Aikman 1976), and the adopted mass ratio, the total mass of this system can be estimated (Heintz 1978) as

$$\mathcal{M}_1 + \mathcal{M}_2 = [a_1(1+r) \sin i]^3 / [P^2(r \sin i)^3] = 5.6 \mathcal{M}_\odot. \quad (9)$$

Thus the masses of the primary and the companion are estimated as  $\mathcal{M}_1 = 3.8 \mathcal{M}_\odot$  and  $\mathcal{M}_2 = 1.8 \mathcal{M}_\odot$ , respectively.

The distance of this system is estimated as  $d_{pc} = (a_1 \sin i)(1 + r)/(ra' \sin i) = 30.5$  pc, with a corresponding parallax  $\pi'' = 0''.033$ . This is within the error range of the trigonometric parallaxes  $\pi'' = 0''.032$  (Hoffleit & Jaschek 1982) and  $0''.0258 \pm 0''.0074$  (van Altena, Lee, & Hoffleit 1991). The linear semi-major axis is thus estimated as 0.73 au, and the absolute magnitudes of the two components are estimated as  $M_{v1} = -0.20$  mag and  $M_{v2} = +1.80$  mag, respectively. From measurements of hydrogen-line absorption (Petrie & Maunsell 1949) and photometry (Eggen 1972), the absolute magnitude of  $\alpha$  And was determined as  $M_{sp} = -0.3 \pm 0.3$  mag and  $M_{ph} = -0.35 \pm 0.2$  mag, which are satisfactorily close to our estimate.

The object  $\alpha$  And has common space motion with the Pleiades cluster and is probably a member of the Pleiades group (Eggen 1972). The colors and luminosities of both components of  $\alpha$  And as determined in this work agree well with the color-magnitude diagram for the Pleiades cluster (Eggen 1965). It is interesting to note that the distance from  $\alpha$  And to the Pleiades cluster is at least 95 pc.

The stellar diameter is estimated (Allen 1983) as

$$\log \theta'' = -2.031 + \log (R/R_{\odot}) - (m_v - M_v + 5)/5, \quad (10)$$

where  $R/R_{\odot}$  is the ratio of the radii of the star and the Sun;  $m_v$  and  $M_v$  are the apparent visual magnitude and the absolute magnitude of the star. For  $\alpha$  And there have been several estimates of its primary radius from measurements of energy distribution and the infrared flux method (Babu 1977; Shallics 1985; Stift 1974). The average value of these estimates,  $R/R_{\odot} = 3.8$ , was adopted for this calculation. For a binary system with spectra B8 IV and A3 V, and with  $m_{v1} = 2.22$  mag and  $M_{v1} = -0.20$  mag, the ratio of the angular diameters of the two components of  $\alpha$  And,  $\theta''_2/\theta''_1$ , is approximately 0.43 (Allen 1983). Thus, the diameters of the two components of  $\alpha$  And are estimated from the above formula as 1.1 and 0.5 mas, respectively. These are the values used in calculating the magnitude difference in § 4.2.

It is important to note that the estimated masses depend critically on the adopted mass ratio. If instead of a value of 0.48, we adopted a value of 0.34, derived from a parallax of  $0''.258$ , the total mass of the system must be closer to  $12 M_{\odot}$  than to  $5.6 M_{\odot}$ , with the primary earlier than B8, perhaps B3, which is closer to the UV spectral type. In both cases, there are inconsistencies between the spectral types estimated from the masses and those estimated from the luminosities. While the consistency with the absolute magnitudes given above is somewhat worse for the case of the smaller mass ratio, the spectroscopic data are not sufficient to choose one solution over the other.

Successful resolution of the spectroscopic binary  $\alpha$  And with the Mark III Stellar Interferometer demonstrates the capability of optical interferometry for binary star astronomy. For observation of close binary stars in particular, it is required to have not only high resolution and good detectability of magnitude difference, but also a reliable, fully automated instrument, in order to obtain many scans per night. For the binary star  $\alpha$  And, all of the orbital parameters have been determined independently at two different optical wavelengths, and are consistent with the results from spectroscopy. The precise measurements of the magnitude differences between the two components, and of the angular size and the inclination of the orbit, lead to estimates of the physical parameters of the system. Further spectroscopic observations for the companion are under way at the Californian Institute of Technology, which will finally verify the estimated physical characteristics of  $\alpha$  And.

Thanks to Wallace L. W. Sargent, California Institute of Technology, for valuable discussions, and to Lu Rarogiewicz for assisting with the observations. Literature survey is based on the SIMBAD data retrieval system, data base of the Strasbourg, France, Astronomical Data Center.

#### REFERENCES

- Abt, H. A., & Snowden, S. M. 1973, *AJS*, 25, 137  
 Adelman, S. J., & Pypert, D. M. 1983, *A&A*, 118, 313  
 Aikman, G. C. L. 1976, *Publ. Dom. Astrophys. Obs.*, 14, No. 18, 379  
 Allen, C. W. 1983, *Astrophysical Quantities* (London: Athlone)  
 Aydin, C., & Hack, M. 1978, *A&AS*, 33, 27  
 Babu, I. E. 1977, *Ap&SS*, 50, 343  
 Baker, R. H. 1908, *Pub. Allegheny Obs.*, 1, 22  
 Batten, A. H., Fletcher, J. M., & MacCarthy, D. G. 1989, *Publ. Dom. Astrophys. Obs.*, 17, 10  
 Colavita, M. M., Shao, M., & Staelin, D. H. 1987, *Appl. Opt.*, 26, 4113  
 Derman, I. E. 1982, *Ap&SS*, 88, 135  
 Eggen, O. J. 1957, *AJ*, 62, 45  
 ———. 1965, *ARA&A*, 3, 235  
 ———. 1972, *ApJ*, 173, 63  
 Hanbury Brown, R. 1974, *The Intensify Interferometer* (London: Taylor and Francis), 122  
 Heintz, W. D. 1978, *Double Stars* (Dordrecht: Reidel), 48  
 Hoffleit, D., & Jaschek, C. 1982, *The Bright Star Catalogue* (4th rev. ed.; New Haven: Yale Univ. Observatory)  
 Hutter, D. J., et al. 1989, *ApJ*, 340, 1103  
 Johnson, H. L., Mitchell, R. I., Iriarte, B., & Wisniewski, W. Z. 1966, *Publ. Lunar & Planet. Lab.*, 4, 99  
 Jugaku, J., & Sargent, W. L. W. 1968, *ApJ*, 151, 259  
 Kohl, O. 1937, *Astron. Nach.*, 262, 472  
 Ludendorff, H. 1908, *Astron. Nach.*, 178, 23  
 Luyten, W. J., Struve, O., & Morgan, W. W. 1939, *Publ. Yerkes Obs.*, 7, Pt. IV, 1  
 McAlister, H. A., & Hartkopf, W. I. 1988, *CHARA Contribution*, No. 2  
 Mozurkewich, D., et al. 1988, *AJ*, 95, 1269  
 Mozurkewich, D., Johnston, K. J., Simon, R. S., Hutter, D. J., Colavita, M. M., Shao, M., & Pan, X. P. 1991, *AJ*, 101, 2207  
 Pan, X. P., Shao, M., Colavita, M. M., Mozurkewich, D., Simon, R. S., & Johnston, K. J. 1990, *ApJ*, 356, 641  
 Pearce, J. A. 1936, *Publ. AAS*, 9, 16  
 Petrie, R. M. 1950, *Publ. Dom. Astrophys. Obs.*, 8, No. 10, 319  
 Petrie, R. M., & Maunsell, C. D. 1949, *Publ. Dom. Astrophys. Obs.*, 8, No. 8, 253  
 Rakos, K. D., Jenker, H., & Wood, J. 1981, *A&AS*, 43, 209  
 Shallics, M. J., Baruch, J. E. F., Booth, A. J., & Selby, M. J. 1985, *MNRAS*, 213, 307  
 Shao, M., et al. 1990, *AJ*, 100, 1701  
 Shao, M., et al. 1988, *A&A*, 193, 357  
 Shao, M., Colavita, M. M., Staelin, D. H., Johnston, K. J., Simon, R. S., Hughes, J. A., & Hershey, J. L. 1987, *AJ*, 93, 1280  
 Smith, R. C. 1983, *Observatory*, 103, 29  
 Stift, M. J. 1973, *A&A*, 22, 209  
 van Altena, W. S., Lee, J. T., & Hoffleit, E. D. 1991, *General Catalogue of Trigonometric Stellar Parallaxes* (New Haven: Yale Univ. Observatory)